



Title	Influence of Preparation Temperatures of V <sub>2</sub> O <sub>5</sub> Powder on Reduction Rate in V <sub>2</sub> O <sub>5</sub> -SO <sub>2</sub> System
Author(s)	Shimizu, Akira; Kawarai, Shuji; Furuichi, Ryusaburo; Ishii, Tadao
Citation	Memoirs of the Faculty of Engineering, Hokkaido University, 17(2), 167-175
Issue Date	1987-12
Doc URL	<a href="http://hdl.handle.net/2115/38024">http://hdl.handle.net/2115/38024</a>
Type	bulletin (article)
File Information	17(2)_167-176.pdf



[Instructions for use](#)

# INFLUENCE OF PREPARATION TEMPERATURES OF V<sub>2</sub>O<sub>5</sub> POWDER ON REDUCTION RATE IN V<sub>2</sub>O<sub>5</sub>-SO<sub>2</sub> SYSTEM

Akira SHIMIZU, Shuji KAWARAI\*, Ryusaburo FURUICHI  
and Tadao ISHII

(Received June 30, 1987)

## Abstract

Reactivity of three V<sub>2</sub>O<sub>5</sub> (V1, V2 and V3) obtained at different preparation temperatures ( $T_p$ ) was compared by their rate of reduction in SO<sub>2</sub> stream of 300 ml/min. The V<sub>2</sub>O<sub>5</sub> samples were prepared by thermal decomposition of NH<sub>4</sub>VO<sub>3</sub> in an air stream of 100 ml/min at 400 (V1), 450 (V2) and 550 °C (V3) for 1 hr. The reduction followed Mampel's equation in a temperature range of 350-400°C. The measured rate was decreased with an increase in  $T_p$ . SEM observation and measurements of interplanar spacing ( $d_{hoo}$ ), peak breadth at half maximum intensity ( $\beta_{hoo}$ ), BET surface area (S), and stretching vibration frequency of V=O( $\nu$ ) of V<sub>2</sub>O<sub>5</sub> were carried out. Values of  $\nu$  and  $d_{hoo}$  were independent of  $T_p$ . Lattice strain  $\eta_a$  and crystallite size  $L_a$  were estimated by Hall's method from  $\beta_{hoo}$ .  $\eta_a$  was decreased with  $T_p$  while  $L_a$  was increased.  $L_a$  agreed with the diameter ( $D_s$ ) calculated from S. The reduction was presumed to proceed on the surface of V<sub>2</sub>O<sub>5</sub> crystallites. The change in the reduction rate with  $T_p$  was considered to depend on the strain energy stored in the crystallite.

## 1. Introduction

In our previous paper<sup>1)</sup> thermal decomposition process of NH<sub>4</sub>VO<sub>3</sub> was studied by gas flow DTA and X-ray technique. It was reported that a single phase of V<sub>2</sub>O<sub>5</sub> crystal was obtained above 400°C and its crystal growth continued extensively up to 550°C. Since the crystallinity of V<sub>2</sub>O<sub>5</sub> was affected by the decomposition temperature of NH<sub>4</sub>VO<sub>3</sub> namely the preparation temperature of the oxide, it was assumed that the reactivity of V<sub>2</sub>O<sub>5</sub> is affected by its preparation temperature. In the present investigation, three V<sub>2</sub>O<sub>5</sub> samples were prepared at 400, 450 and 550 °C by thermal decomposition of NH<sub>4</sub>VO<sub>3</sub>. The changes in the reactivity of these V<sub>2</sub>O<sub>5</sub> powders was investigated on the basis of the formation rate of V<sub>4</sub>O<sub>9</sub>, which is considered to have the closest resembling structure to that of V<sub>2</sub>O<sub>5</sub> among all intermediate oxides formed in the course of the reduction of V<sub>2</sub>O<sub>5</sub> with SO<sub>2</sub><sup>2,3)</sup>.

## 2. Experimental

### 2.1 Material

Three V<sub>2</sub>O<sub>5</sub> (V1, V2 and V3) samples were prepared by thermal decomposition of NH<sub>4</sub>

$\text{VO}_3$  ( $-250$  mesh)<sup>1)</sup>. A commercial  $\text{NH}_4\text{VO}_3$  ( $2\text{g}$ ) (Kanto Chemical Co. Reagent Grade) was heated in a horizontal electric furnace with a quartz tube ( $\phi=10\text{ mm}$ ) at an air flow rate of  $100\text{ ml/min}$  for  $1\text{ hr}$  at  $400$  (V1),  $450$  (V2) and  $550\text{ }^\circ\text{C}$  (V3), respectively. X-ray diffraction patterns of these  $\text{V}_2\text{O}_5$  coincided with ASTM card<sup>4)</sup>. SEM photographs of these samples are shown in Fig. 1. Particle size distribution of the samples were in the range of  $1$  to  $10\text{ }\mu\text{m}$  and showed no relation to the preparation temperatures.

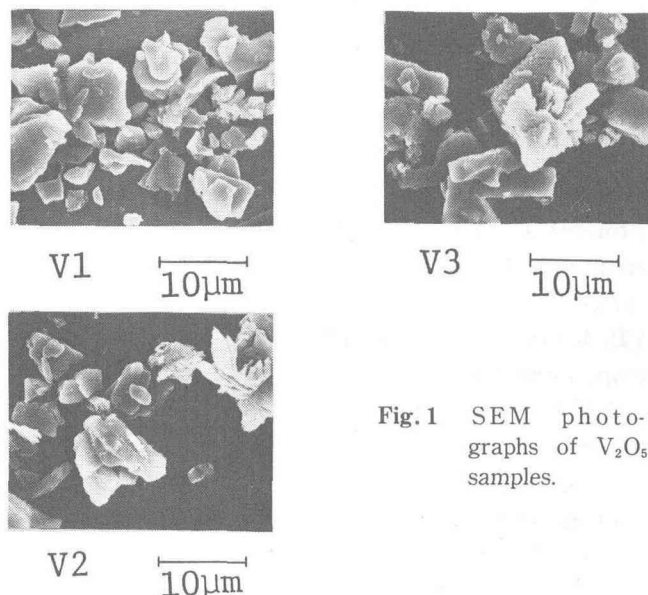


Fig. 1 SEM photographs of  $\text{V}_2\text{O}_5$  samples.

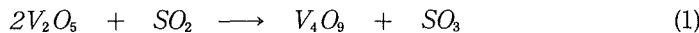
## 2.2 Reaction method

The reduction of  $\text{V}_2\text{O}_5$  sample ( $100\text{ mg}$ ) was carried out in the quartz reaction tube ( $\phi=10\text{ mm}$ ) placed in a vertical electric furnace. The sample powder was supported by spreading it on a quartz wool layer packed in the tube.  $\text{SO}_2$  gas was introduced at a constant flow rate into the reaction tube from a gas bomb (purity: 99.1%). The gas was dried by passing the gas through a drying agent ( $\text{P}_2\text{O}_5$ ). The fractions of  $\text{V}_2\text{O}_5$  reduced ( $\alpha$ ) were  $0.07$ ,  $0.23$ ,  $0.21$  and  $0.22$  when sample V2 was reduced at  $400\text{ }^\circ\text{C}$  for  $2\text{ hr}$  under  $\text{SO}_2$ -flow rates of  $100$ ,  $200$ ,  $300$  and  $400\text{ ml/min}$ , respectively. These  $\alpha$ -values show that the effect of laminar film between gas and particle is constant over a flow rate of  $200\text{ ml/min}$ . Accordingly, subsequent experiments were carried out at  $\text{SO}_2$  flow rate of  $300\text{ ml/min}$ . X-ray diffraction patterns of the mixed phase of  $\text{V}_2\text{O}_5$  and  $\text{V}_4\text{O}_9$  was obtained after the reduction of  $\text{V}_2\text{O}_5$  samples for  $5\text{ hr}$  in a temperature range of  $350$ - $400\text{ }^\circ\text{C}$ . This fact is consistent with the result reported by Taniguchi et al<sup>2)</sup> for the formation temperature of  $\text{V}_4\text{O}_9$  ( $320$ - $430\text{ }^\circ\text{C}$ ). Then the reduction was carried out for  $1$  to  $5\text{ hr}$  at the temperatures of  $350$ ,  $375$  and  $400\text{ }^\circ\text{C}$ .

## 2.3 Measurment of fractional conversion ( $\alpha$ )

In order to determine the fraction of  $\text{V}_2\text{O}_5$  reduced ( $\alpha$ ), the concentration ratio of vanadium ions,  $[\text{V}^{4+}] / \{ [\text{V}^{4+}] + [\text{V}^{5+}] \}$  was measured according to JIS<sup>5)</sup> by means of potentiometric titration of Mohr's salt solution. After the reaction for a fixed time,  $50\text{ mg}$

of sample was dissolved in 100 ml of 3N-H<sub>2</sub>SO<sub>4</sub>. The 10 ml of this solution was mixed with 10 ml of conc. H<sub>3</sub>PO<sub>4</sub> and diluted to 100 ml with water and then titrated by 1/30N-Mohr's salt solution. The titration volume was represented by V<sub>1</sub> (ml). After the titration, V<sup>4+</sup> ion in the solution was oxidized into V<sup>5+</sup> by 0.1N-KMnO<sub>4</sub>. The solution was titrated once again by the Mohr's salt solution. This second titration volume was represented by V<sub>2</sub> (ml). Since V<sub>2</sub>-V<sub>1</sub> is equivalent to the [V<sup>4+</sup>] and the reduction process is formulated as eq. (1),



the fractional conversion ( $\alpha$ ) is represented by

$$\alpha = 2(V_2 - V_1)/V_2 \quad (2)$$

#### 2.4 X-ray diffraction

X-ray powder diffractometer (Rigakudenki Co. Type 2142) was used for identification of the samples before and after the reaction. The diffraction peak breadth at half-maximum intensity<sup>7)</sup> and the interplanar spacing were measured from the diffraction peak profile. The profile was obtained by the manual step scan method. The scan was carried out by moving the goniometer every 1/100 degrees. The diffraction intensities were counted five times for 10 sec at the each angle. The standard sample of V<sub>2</sub>O<sub>5</sub>, which was prepared by calcining V3 at 650 °C for 24 hr in air, and that of  $\alpha$ -Al<sub>2</sub>O<sub>3</sub>, which was prepared by calcining activated alumina at 1300 °C for 3 hr, were used for the estimation of the peak breadth and the interplanar spacing, respectively. Cu-target was used in the former case and Cr-target in the latter.

#### 2.5 IR measurement

The stretching vibration of V=O group was measured by KBr disk method, using IR spectrometer (Shimazu Co. 430). The disk was prepared by pressing the mixture of 0.1 mg of sample and 200 mg of KBr powder at a pressure of 5.3 ton/cm<sup>2</sup>.

#### 2.6 SEM observation

The particle of samples was observed by SEM (JEOL T-20). The sample was dispersed in ethanol by ultrasonic wave generator and then sedimented on the sample holder (Aluminum disk  $\phi=15$  mm). The surface of the sample was coated with a gold film in vacuum evaporator to prevent electrification.

#### 2.7 BET surface area measurement

The surface area was calculated by BET equation from the amount of adsorbed Ar at -197 °C. Before the adsorption, the sample (0.4g) was evacuated at 10<sup>-4</sup> mmHg for 10 hr at room temperature.

### 3. Result and discussion

As shown in Fig. 2, the reduction rate of three V<sub>2</sub>O<sub>5</sub> (V1, V2 and V3) is found to follow Mampel's equation<sup>8)</sup> (eq. (3)), which is based on an assumption that the rate controlling step is the phase-boundary reaction.

$$1 - (1 - \alpha)^{1/3} = k_M t \quad (3)$$

It may be observed from the slopes of the straight lines of Fig. 2 that the lower the preparation temperature of V<sub>2</sub>O<sub>5</sub> is, the larger the k<sub>M</sub>-value is. Table 1 shows the values of k<sub>M</sub> and activation energies (E<sub>a</sub>) of three V<sub>2</sub>O<sub>5</sub>. X-ray diffraction revealed that the samples obtained in the course of the reaction were a mixture of V<sub>2</sub>O<sub>5</sub> and V<sub>4</sub>O<sub>9</sub>.

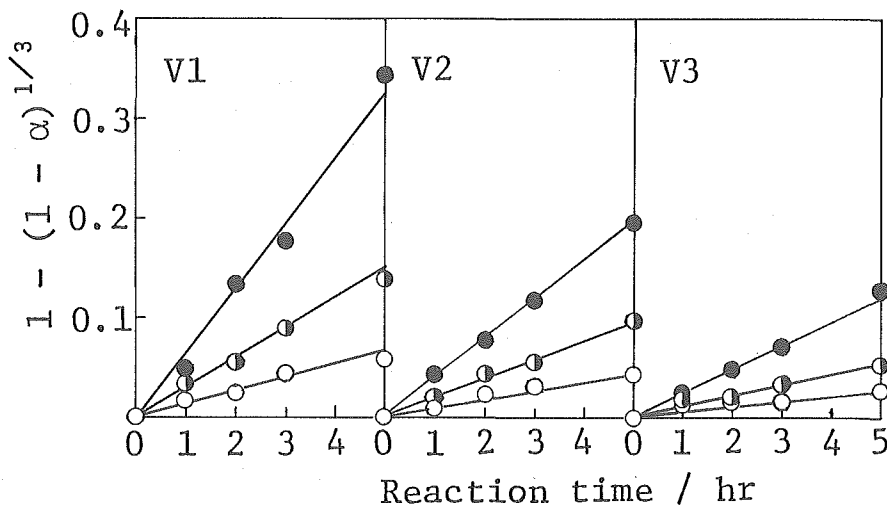


**Fig. 2** Plots of  $1 - (1 - \alpha)^{1/3}$  vs. time for reaction of  $\text{V}_2\text{O}_5$  samples.  
Reaction temperature, ○: 350°C, ◑: 375°C, ●: 400°C.

**Table 1** Reaction rate constants ( $k_M$ ) and activation energies ( $E_a$ ).

Sample	Reaction temperature/°C	$k_M/\text{hr}^{-1}$	$E_a/\text{kcal} \cdot \text{mol}^{-1}$
V1	350	$1.36 \times 10^{-2}$	27
	375	$3.00 \times 10^{-2}$	
	400	$6.93 \times 10^{-2}$	
V2	350	$9.20 \times 10^{-3}$	26
	375	$1.90 \times 10^{-2}$	
	400	$3.90 \times 10^{-2}$	
V3	350	$5.60 \times 10^{-3}$	25
	375	$1.02 \times 10^{-2}$	
	400	$2.30 \times 10^{-2}$	

**Table 2** Interplanar spacing ( $d_{hkl}$ ), peak breadth at half-maximum intensity ( $\beta_{hkl}$ ) and specific surface area ( $S$ ).

Sample	V1	V2	V3
$d_{hkl}/\text{\AA}$			
$d_{600}$	1.918	1.918	1.918
$d_{400}$	2.883	2.883	2.883
$d_{200}$	5.773	5.773	5.774
$\beta_{hkl}/\text{deg}$			
$\beta_{600}$	0.097	0.057	0.038
$\beta_{400}$	0.075	0.045	0.032
$\beta_{200}$	0.057	0.030	0.021
$S/\text{m}^2 \cdot \text{g}^{-1}$	7.4	5.6	3.5

Table 2 shows the interplanar spacing ( $d_{600}$ ,  $d_{400}$  and  $d_{200}$ ) and peak breadth at half maximum intensity ( $\beta_{600}$ ,  $\beta_{400}$  and  $\beta_{200}$ ) of three crystal faces aligned in the direction of a-axis, and specific surface areas ( $S$ ). The difference in  $d_{hoo}$ -values is not observed between the samples. On the other hand,  $\beta_{hoo}$ -value decreases with an increase in the preparation temperature. It is suggested from the change in  $\beta_{hoo}$  that the crystallinity of V<sub>2</sub>O<sub>5</sub> increases with its preparation temperature. The surface area ( $S$ ) correspondingly decreases with the preparation temperature. From SEM photographs of V3 in Fig. 1 and an assumption that the particle of sample is cubic, the average size of the particle was measured to be 5  $\mu\text{m}$ , which lead to a calculation of the surface area of 0.35  $\text{m}^2/\text{g}$  by using the density of V<sub>2</sub>O<sub>5</sub> (3.4  $\text{g}/\text{cm}^3$ ). This is much smaller than the BET area of 3.5  $\text{m}^2/\text{g}$  measured for V3. The discrepancy leads to a conclusion that every particle of the sample consists of many small particles. Fig. 3 shows the magnified SEM photographs of V1, V2 and V3. It is observed that many smaller particles combine with each other and build up the large particles of the sample. Furthermore, the size of the smaller particle is observed to increase with the preparation temperature. The average size of the samller particle was estimated to be  $5.2 \times 10^3 \text{ \AA}$  in the case of V3 which shows the smaller particles most clearly.

From the BET specific surface area, the particle diameter ( $D_s/A$ ) is calculated by eq. (4), when the shape of V<sub>2</sub>O<sub>5</sub> sample is spherical or cubic

$$D_s = 6 \times 10^4 / d_s \cdot S \quad (4)$$

where  $d_s$  is the density of V<sub>2</sub>O<sub>5</sub> (3.4  $\text{g}/\text{cm}^3$ ).  $D_s$ -values calculated are shown in Table 3, assuming that  $d_s$ -value is constant even if the preparation temperature is changed.  $D_s$ -value of V3 is  $5.0 \times 10^3 \text{ \AA}$  which is fairly consistent with the average size ( $5.2 \times 10^3 \text{ \AA}$ ) of the smaller particles estimated from SEM photograph in Fig. 3. Since the molecular diameter of SO<sub>2</sub>, which is the reducing agent, is almost same as that of Ar ( $3.8 \text{ \AA}$ )<sup>10</sup> which is the adsorbate for the BET experiment, it is reasonable to expect that the reaction between V<sub>2</sub>O<sub>5</sub> and SO<sub>2</sub> takes place on the surface of smaller particles building up the large particles of V<sub>2</sub>O<sub>5</sub>.

In order to investigate the influence of the size of larger particles on the reduction rate, two sample powders of different particle sizes (100-150 and 250-325 mesh) were obtained by sieving a commercial V<sub>2</sub>O<sub>5</sub> (Nakarai Chemical Co., Reagent Grade). The particle structure of the commercial V<sub>2</sub>O<sub>5</sub> was found to be similar to that of V3 from the magnified SEM photograph in Fig. 3. The classification by sieving of prepared V<sub>2</sub>O<sub>5</sub> samples was unsuccessful, because the size of large particles was smaller than 10  $\mu\text{m}$  as seen in Fig. 1. The fractional conversions ( $\alpha$ ) of two groups of commercial V<sub>2</sub>O<sub>5</sub> were almost the same;  $\alpha=0.16$  and 0.14, respectively, at the reaction temperature of 400 °C and the reaction time of 1 hr. These  $\alpha$ -values show that the reduction process is not affected by the size of larger particles. This fact supports the previous expectation that SO<sub>2</sub> gas is supplied sufficiently on the surface of smaller particles and the reduction takes place on them.

According to Hall<sup>10</sup>, the peak breadth at half maximum intensity ( $\beta_{hoo}$ ) in Table 2 is represented by two terms, that is, the crystallite size ( $L_a$ ) and the lattice strain of crystallite ( $\eta_a$ ) as in the following (eq. (5)).

$$\beta_{hoo} \cos\theta/K\lambda = 1/L_a + \eta_a \sin\theta/K\lambda \quad (5)$$

where  $\lambda$  is the wave length of X-ray,  $\theta$  is Bragg's angle and  $K$  is the shape factor (0.9).  $L_a$

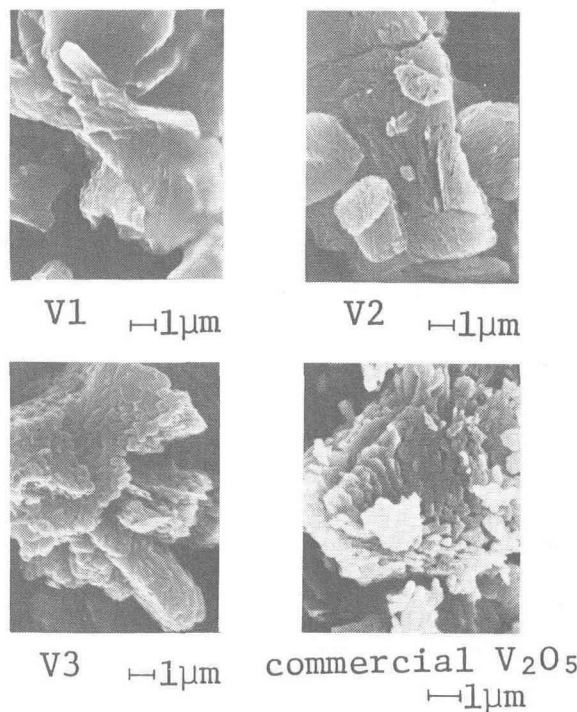


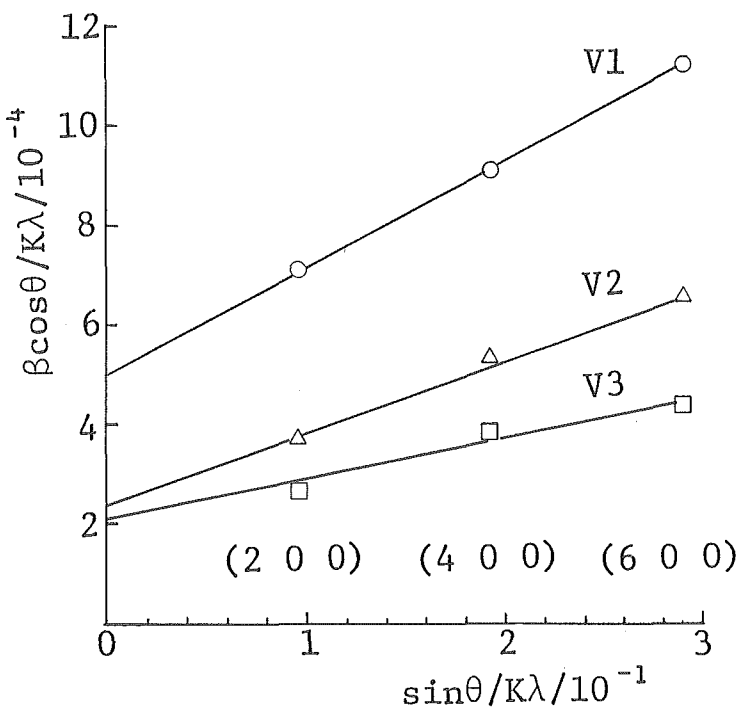
Fig. 3 SEM photographs of  $\text{V}_2\text{O}_5$  crystallites.

and  $\eta_a$  correspond to the values for the direction of a-axis, because X-ray diffraction peaks were observed for (600), (400) and (200) face. The plot of eq. (5) by using  $\beta_{h00}$ -values in Table 2 give the straight lines as shown in Fig. 4.  $\eta_a$  and  $L_a$  obtained are listed in Table 3. The order of  $\eta_a$  is  $\mathbf{V1} > \mathbf{V2} > \mathbf{V3}$  and that of  $L_a$  is  $\mathbf{V3} > \mathbf{V2} > \mathbf{V1}$ . The orders of  $\eta_a$  and  $L_a$  indicate that the increase in preparation temperature of  $\text{V}_2\text{O}_5$  results in the larger crystallite size and the smaller lattice strain; in other words, the increased crystallinity, the higher regularity of crystal lattice and the more uniform size of unit cells which form the crystallites. As seen in Table 2, three samples show similar  $d_{h00}$ -values, in contrast to different  $\eta_a$ . Since  $\eta_a$  corresponds to the distribution of interplanar spacing ( $\langle \Delta d/d \rangle$ ), the calculated value of  $\Delta d$  ( $= \eta_a \cdot d_{h00}$ ), the displacement of (h00) faces, is found to be in the range of  $4.1 \times 10^{-3} \sim 12.4 \times 10^{-3}\ \text{\AA}$  for **V1**,  $1.9 \times 10^{-3} \sim 8.1 \times 10^{-3}\ \text{\AA}$  for **V2** and  $1.5 \times 10^{-3} \sim 4.6 \times 10^{-3}\ \text{\AA}$  for **V3**, respectively. As seen in Table 3,  $L_a$  agrees with  $D_s$  approximately. Moreover, as described earlier  $D_s$  for **V3** also agreed with the average size ( $5.2 \times 10^3\ \text{\AA}$ ) of small particles estimated from SEM photograph in Fig. 3. These agreements in the sizes suggest that the small particle seen in Fig. 3 corresponds to the crystallite of  $\text{V}_2\text{O}_5$  sample.

As mentioned above, the reduction of  $\text{V}_2\text{O}_5$  takes place on the surface of its small particles, that is, crystallites and the rate is controlled by the phaseboundary reactions (eq. (3)). The reaction rate for one crystallite is represented by eq. (6),

$$-\frac{dw}{dt} = k_0 s C \quad (6)$$

where  $w$  and  $s$  are the weight and the surface area of one crystallite,  $k_0$  is the rate constant and  $C$  is the concentration of  $\text{SO}_2$  on the surface of the crystallite. When the total weight

Fig. 4 Hall's plots of V<sub>2</sub>O<sub>5</sub> samples.**Table 3** Particle diameter ( $D_s$ ) calculated from surface area, crystallite size ( $L_a$ ) and lattice strain ( $\eta_a$ ).

Sample	$D_s/A$	$L_a/A$	$\eta_a/$
V1	$2.4 \times 10^3$	$2.0 \times 10^3$	$2.15 \times 10^{-3}$
V2	$3.2 \times 10^3$	$4.0 \times 10^3$	$1.40 \times 10^{-3}$
V3	$5.0 \times 10^3$	$4.8 \times 10^3$	$8.00 \times 10^{-4}$

of sample is  $W$ , the rate is represented by eq. (7) assuming that the crystallite is cubic and the size is  $D_s$ ,

$$-dW/dt = (6k_0 W_0^{1/3}/d_s \cdot D_s) C W^{2/3} \quad (7)$$

where  $W_0$  is the total weight of the sample before the reaction. Eq. (9) is obtained by integrating eq. (7) and by introducing the fractional conversion ( $\alpha$ ) in eq. (8).

$$\alpha = 1 - W/W_0 \quad (8)$$

$$1 - (1 - \alpha)^{1/3} = (6k_0 \cdot C / d_s \cdot D_s) t \quad (9)$$

Then the rate constant  $k_M$  of Mampel's equation (eq. (3)) is represented by eq. (10).

$$k_M = 6k_0 \cdot C / d_s \cdot D_s \quad (10)$$

The density  $d_s$  can be assumed to be constant. The value of  $C$  is also constant, when SO<sub>2</sub> flow rate is 300 ml/min. Thus, it is considered that the difference of  $k_M$  in Table 1 is ascribed to that of  $k_0$  and  $D_s$ . In order to compare  $k_0$ -values for the samples, the value of

$k_M \cdot D_s$  was calculated, which is proportional to  $k_0$ . As seen in Table 4, the order of  $k_M \cdot D_s$  is V1 > V2 > V3 at three reaction temperatures. Since the value of  $k_0$  corresponds to the reaction rate per surface area of the crystallite, it will depend upon the lattice distortion of  $V^{5+}$  and  $O^{2-}$  or the bond strength between them. It has been reported that the removal of oxygen layer of (020) face plays an important role in the reduction. The IR band of  $V=O$  bond ( $\nu$ ) was measured in order to examine the influence of the preparation temperature of  $V_2O_5$  on the bond strength. As seen in Fig. 5, three samples show the absorption spectra at  $1020\text{ cm}^{-1}$ , and the difference in  $\nu$  is not detected among them. On the other hand, the difference could be found in  $\eta_a$ -value which depends upon the degree of the lattice distortion as mentioned above, and its order is consistent with that of  $k_0$ -value. Therefore it is

Table 4  $k_M \cdot D_s$  ( $\propto k_0$ ) values of eq. (10).

Sample Reaction temp./°C	$k_M \cdot D_s / A \cdot hr^{-1}$		
	V1	V2	V3
350	$3.26 \times 10$	$2.94 \times 10$	$2.80 \times 10$
375	$7.20 \times 10$	$6.08 \times 10$	$5.10 \times 10$
400	$1.66 \times 10^2$	$1.25 \times 10^2$	$1.15 \times 10^2$

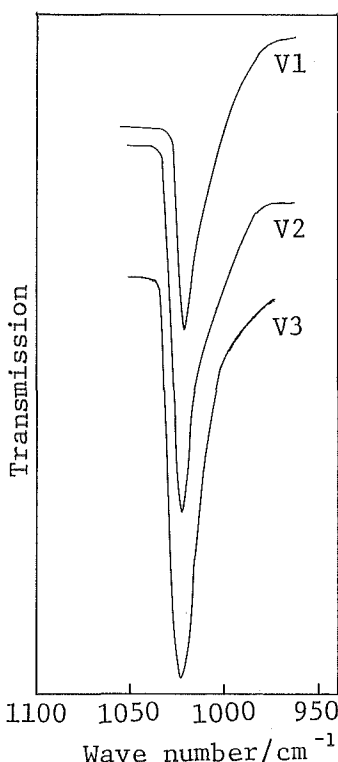


Fig. 5 IR spectra of  $V_2O_5$  samples.

considered that  $k_0$ -value depends on the difference in the strain energy accumulating in the samples.

#### Acknowledgment

The authors are very grateful to Professor T. Morozumi for obtaining the SEM photographs of the samples.

#### Reference

- 1) A. Shimizu, R. Furuichi and T. Ishii, J. Chem. Soc. Jap. Chemistry and Industrial Chemistry, **1**, 39 (1975).
- 2) M. Taniguchi, A. Miyazaki and H. Yokomizo, Catalyst, **10**, 99 (1968).
- 3) K. Kawashima, K. Kosuge and S. Kachi, Chem. Lett., 1131 (1975).
- 4) ASTM Card 9-387.
- 5) ASTM Card 23-724.
- 6) JIS, G 1221 (1981).
- 7) S. F. Bartram, "Hand book of X-rays", McGraw-hill (1967) 17-9.
- 8) K. Mampel, Z. Phys. Chem., **A** 187, 43 (1940).
- 9) D. W. Breck, "Zeolite Molecular Sieve", John Willy and Sons. (1974) p636.
- 10) W. H. Hall, Proc. Phys. Soc., **A** 62, 741 (1949).